



NLRP12-associated autoinflammatory disease: A novel causal mutation and bioinformatics analyses

Zhonghua Li^{a,b,1}, Qi Zhi^{c,1}, Jiahuang Li^{a,*}, Bo Zhu^{a,*}

^a School of Biopharmacy, China Pharmaceutical University, Nanjing 211198, PR China

^b School of Basic Medicine and Clinical Pharmacy, China Pharmaceutical University, Nanjing 211198, PR China

^c Department of Radiology, Affiliated Hospital of Nanjing University of Chinese Medicine, Nanjing 210029, PR China

ARTICLE INFO

Keywords:

NLRP12

NLRP12-AID

Gene mutation

Single-cell sequencing

Molecular docking

ABSTRACT

Nucleotide-binding leucine-rich repeat-containing receptor 12-associated autoinflammatory disease (NLRP12-AID) is a rare autosomal dominant disorder. In this study, we reported a case of this rare disease with a novel NLRP12 mutation (A218V, rs749659859). The patient displayed typical symptoms, including recurrent fever, arthralgia, and skin allergies. Elevated serum IgE, decreased apolipoprotein A1, high-density lipoprotein cholesterol, and fluctuating levels of various leukocyte subtypes, procalcitonin, IL6, creatine kinase, and 25-hydroxyvitamin D were also detected. Inflammatory lesions were observed in multiple organs using ¹⁸F-FDG PET/CT. By mining single-cell transcriptome data, we identified relatively high expression of NLRP12 in monocytes compared to other human peripheral blood mononuclear cells. NLRP12-positive monocytes exhibited reduced expression of *IL18*, *CCL3*, and *TNFA* compared to NLRP12-negative monocytes. Structural analyses suggested that the A218V mutation, along with A218T and F402L, may reduce the ATP-binding affinity of the NLRP12 protein. These findings may provide new insights into the mechanisms of NLRP12-AID, and suggest the potential ATP-based therapy for further investigation.

1. Introduction

Recent studies have indicated that NLRP12 mutations can result in NLRP12-associated autoinflammatory disease (NLRP12-AID), a rare autosomal dominant AID also recognized as familial cold autoinflammatory syndrome 2 (FCAS2) [1,2]. NLRP12-AID is primarily activated by cold exposure, and the most significant clinical indication of NLRP12-AID is non-infectious reoccurring fever joined by inflammatory reactions in various tissues including the skin, digestive tract, joints, muscles, and nerves [3].

Diagnosing of NLRP12-AID relies on the detection of mutation in the NLRP12 gene. As far as we know, only 89 cases of NLRP12-AID have been reported worldwide. Previously documented NLRP12 mutation sites associated with NLRP12-AID include p.F402L (c.1206C > G), p.R284* (c.850C > T), p.R35C (c.1054C > T), c.2072 + 3insT, p.D294E (c.882C > G), p.H304Y (c.910C > T), p.W408* (c.1233G > A), and p.G52S (c.154G > A) [4]. Due to its rarity, the pathological mechanism of NLRP12-AID remains unclear. The identification of new NLRP12 pathogenic mutations holds significant clinical implications.

In this study, we reported a new case of NLRP12 mutation (A218V, rs749659859) that triggers NLRP12-AID. Single-cell transcriptome analysis and molecular docking were performed to explore potential mechanisms underlying this rare disease.

2. Methods

2.1. Literature review

We searched the Pubmed database for literature on NLRP12-AID, covering the first reported case in February 2008 through February 2023 using specific search terms, including: “nucleotide-binding oligomerization domain-like receptors family pyrin domain containing 12”, “NLR family pyrin domain containing 12”, “NLRP12”, “NALP12”, “familial cold autoinflammatory syndrome 2”, “FCAS2”, “monarch-1”, “NLRP12-autoinflammatory disease”, “NLRP12-AID”, “autoinflammatory disease”, and “AID”. We summarized the clinical manifestations of NLRP12-AID based on these reports. The mutation sites associated with NLRP12-AID were then analyzed via the VarSome database [34 and

* Corresponding authors.

E-mail addresses: lijiah@cpu.edu.cn (J. Li), zhubo@cpu.edu.cn (B. Zhu).

¹ These authors contributed equally to this work.

<https://doi.org/10.1016/j.clim.2024.110278>

Received 7 February 2024; Accepted 12 June 2024

Available online 13 June 2024

1521-6616/© 2024 Elsevier Inc. All rights are reserved, including those for text and data mining, AI training, and similar technologies.

visualized using the G3viz v1.1.5 and maftools v2.16.0 R packages [35:36].

2.2. Routine blood test, inflammation index calculation, and cytokine detection

White blood cell classification and counting were performed using an automated hematology analyzer. Serum IL6 and IgE levels were measured by enzyme-linked immunosorbent assay (ELISA). Serum procalcitonin (PCT) and 25-hydroxyvitamin D (25(OH)D) levels were determined by chemiluminescence analysis. Serum apolipoprotein A1 (ApoA1) levels were determined by immunoturbidimetric assay. Serum alkaline phosphatase (ALP), lactate dehydrogenase (LDH) and creatine kinase (CK) levels were measured by enzymatic kinetic assay. Serum high-density lipoprotein cholesterol (HDL—C) levels were measured using the homogeneous assay. Four inflammatory indexes were calculated as follows: neutrophil-to-lymphocyte ratio (NLR) = neutrophil count/lymphocyte count; platelet-to-lymphocyte ratio (PLR) = platelet count/lymphocyte count; lymphocyte-to-monocyte ratio (LMR) = lymphocyte count/monocyte count; systemic immune-inflammation index (SII) = (neutrophil count × platelet count)/lymphocyte count [37–39].

2.3. Diagnostic provocation test for chronic inducible urticaria syndrome

A diagnostic provocation test for chronic inducible urticaria syndrome on the patient was performed as previously reported [40]. Briefly, the test consisted of lightly stroking the volar aspect of the forearm with a tongue depressor, and the patient's skin reactions were observed and photographed at five, 10, and 30 min. A positive result was defined as the induction of a linear wheal-flare reaction at the site of the stroke.

2.4. Positron emission tomography/computed tomography (PET/CT) imaging

The PET/CT scan was conducted following a six-hour fast, abstinence from sugary beverages, and attainment of normal blood glucose levels. The patient was administrated 0.15 mCi/kg of ¹⁸F-FDG intravenously and underwent whole-body PET/CT imaging after resting for one hour. CT images were captured in three dimensions for attenuation correction before PET acquisition. The PET images, CT images, and PET/CT fusion images were reconstructed using the TOF-True X method. Two physicians independently reviewed the examination results.

2.5. Whole-exome sequencing and sanger sequencing validation

Genomic DNA was extracted from the blood sample and then fragmented. Libraries were prepared for whole-exosome sequencing using a BGI V4 chip to capture and enrich DNA from target gene exons and adjacent splice regions. The MGISEQ-2000 sequencing platform was utilized for mutation detection. An average effective sequencing depth of at least 100× in the target region and a proportion of sites with an average depth of >20× in the target region of >95% were used as quality control indicators. The sequencing fragments were aligned with the human reference genome (UCSC hg19), and duplicates were subsequently removed. Using the Genome Analysis Toolkit, we conducted base quality score recalibration, single nucleotide variants (SNV), insertion and deletion detection, as well as genotype detection.

The *NLRP12* variant sequence of the patient was further determined via Sanger sequencing and compared to the wild-type human *NLRP12* sequence (NM_144687.4) from the NCBI database using Snapgene software v6.1.1. All sequencing for this study was conducted by the Beijing Genomics Institute (Beijing, China).

2.6. Single-cell RNA sequencing data mining

The GSE158055 dataset was obtained from the GEO database (<http://www.ncbi.nlm.nih.gov/geo/>). We utilized the integrated h5 files uploaded by the original authors of the dataset to obtain a subset of cells from the PBMC sample type, resulting in 126,799 cells [41]. We conducted quality control by excluding cells with <200 detected genes and with genes expressed in less than three cells, along with cells having over 5% mitochondrial genes. Cells with identified genes above 2500 were also eliminated to prevent potential doublets. A total of 118,948 cells and 23,582 genes remained for downstream expression pattern analysis. Single-cell GSEA analysis was performed based on the Gene Ontology Biological Process 2021 gene set. These analyses were executed in Python employing the following software: Scanpy v1.7.2, NumPy v1.23.4, pandas v1.5.1, and GSEAPy v1.0.2 [42:43].

2.7. Molecular modeling, docking, and analysis

We used the trRosetta server (<https://yanglab.nankai.edu.cn/trRosetta/>) to generate the structural coordinates of human NLRP12 [44–46]. The ATP structure was extracted from the NAI5P5 complex crystal structure and optimized using MOE2020.09 with MMFF94X force field. Protein preparation with AMBER99 forcefield and default rigid docking protocol of MOE2020.09 was used for docking ATP into NLRP12. The top 100 poses were refined using the GBVI/WSA DG scoring function based on the London DG scoring function. NLRP12 mutants, including A218V, A218T, and F402L, were constructed using the Design module of MOE2020.09. Structural optimization was performed on wild-type and mutant complexes with MOE2020.09. The Protein Plus (<https://proteins.plus/>) was used to calculate the binding pocket volume, and the PRODIGY server (<https://bianca.science.uu.nl/prodigy/lig>) was used to predict the ligand binding energy. Analysis and visualization of the structures were done using MOE and Discovery Studio 2020 Client.

2.8. Statistical analysis

All statistical analyses were conducted using the R package stats version 4.2.1. To compare cytokine expression levels between two cell subpopulations for single-cell RNA-seq data analysis, a Wilcoxon rank sum test was performed. A *P* value <0.05 was considered statistically significant.

2.9. Study approval

This study adhered to the ethical guidelines of the Declaration of Helsinki, and was approved by the Ethics Committee of China Pharmaceutical University. Written informed consent was obtained from the patient for publication of this article.

2.10. Data availability

The single-cell transcriptome data used to support the findings of this study are available from the GEO database (<https://www.ncbi.nlm.nih.gov/geo/>).

3. Results

3.1. Summary of 89 reported cases of *NLRP12*-AID

Clinical features and mutation information of 89 previously reported *NLRP12*-AID patients are summarized in Fig. 1A and Table S1 [3–27]. Among these patients, almost half had a familial history (36, 40%), with over a third being triggered by cold exposure (33, 37%). The majority experienced periodic fever (69, 78%). The most prevalent symptoms were related to the skin and mucosa (68, 76%) and the motor systems

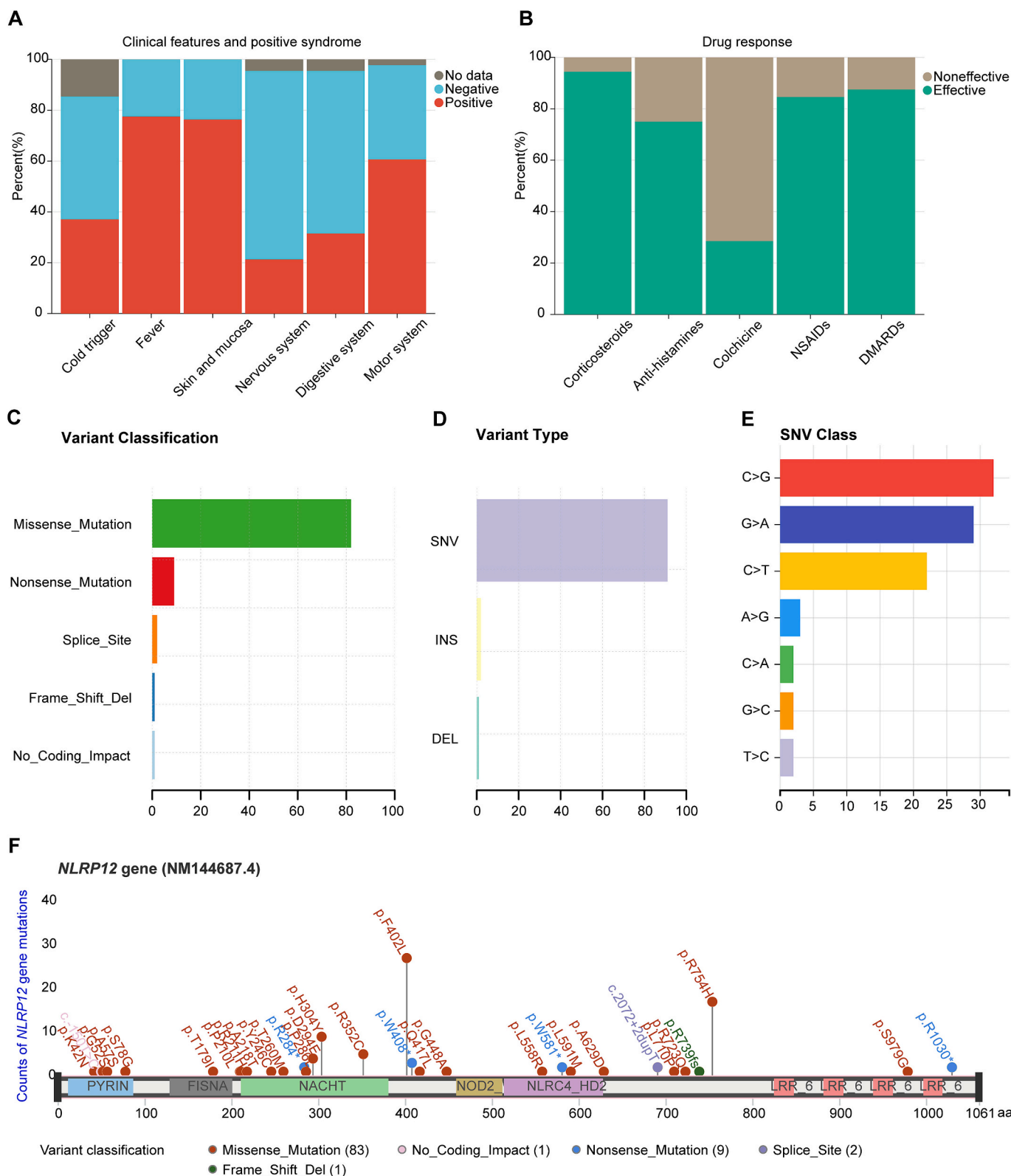


Fig. 1. Clinical symptoms, responses to drug therapy, and mutational characteristics of 89 reported patients with NLRP2-AIDs. (A) Percentage of NLRP2-AID patients with various clinical symptoms. (B) Percentage of NLRP2-AID patients with responsiveness to various drugs. (C–F) All reported NLRP2 gene mutation information from previous literature was compiled, classified, and visualized. (C) Variant Classification, (D) Variant Type, (E) SNV Class, (F) Amino acid change lollipop plot of NLRP2 mutation sites. SNV: single nucleotide variant; INS: insertion; DEL: deletion; NSAIDs: non-steroidal anti-inflammatory drugs; DMARDs: disease-modifying antirheumatic drugs.

(54, 61%) (Fig. 1A). The most effective treatments included corticosteroids (34, 94%), disease-modifying antirheumatic drugs (DMARDs) (7, 88%), non-steroidal anti-inflammatory drugs (NSAIDs) (22, 85%), and anti-histamines (3, 75%). Only a small portion of patients showed a positive response to colchicine therapy (4, 29%) (Fig. 1B).

A majority of these patients expressed missense mutations (77, 87%), while a minority exhibited nonsense mutations (Fig. 1C). SNVs constituted a vast majority of the mutations (Fig. 1D), with the most common base changes being C > G, G > A, and C > T (Fig. 1E). We found that most mutation sites were located in the NACHT domain, whereas a minority were located in the pyrin domain (Fig. 1F).

3.2. The clinical characteristics and imaging manifestations of the patient with the *NLRP12* (A218V) mutation

The study presents the case of a 21-year-old Han Chinese male who has suffered periodic fevers of unknown origin since birth. The fever episodes lasted for one to two weeks and recurred at intervals ranging from one month to several months, occasionally at intervals of one to two weeks. The worst fever of unknown origin was recorded when he was 19 years old with a temperature of 39.4 °C. The attack manifested symptoms of chills, fatigue, dizziness, nausea, sore throat, joint pain affecting the interphalangeal and bilateral knee joints, and occasional swelling of interphalangeal joints (Fig. 2A). The patient also experienced coughing episodes with the production of white mucus sputum which was difficult to expel. The patient had a history of frequent allergies since childhood, which led to episodes of pruritus, erythema, and rash (Fig. 2B). Exposure to cold temperatures could trigger a rash with symptoms similar to urticaria (Fig. 2C-D). The patient had multiple positive skin test reactions to penicillin and was allergic to intravenous acyclovir and ganciclovir. In addition, the patient developed a rash with alcohol exposure. In June 2012, the patient underwent an exploratory laparotomy and appendectomy for abdominal pain, which was diagnosed as appendicitis. Due to focal nodular hyperplasia, the patient had a partial hepatectomy in January 2019.

Using whole-exome sequencing, we found a new heterozygous mutation in *NLRP12*: c.653C > T, p.A218V. Sanger sequencing demonstrated that this mutation was inherited from his mother (Fig. 2E, F). The patient's mother had allergies, resulting in rash and itchy skin, but her symptoms were milder. PET/CT scanning during the attack period (Fig. 2G-R) indicates that the patient presented with right maxillary sinusitis (Fig. 2I), bilateral cervical lymphadenitis (Fig. 2J), bilateral mild axillary lymphadenitis (Fig. 2K), gastroenteritis (Fig. 2L, M), retroperitoneal and bilateral inguinal lymphadenitis (Fig. 2N, O), subcutaneous inflammation in the right lower abdomen and left buttock (Fig. 2P, Q), and bone marrow reactive changes (Fig. 2R).

3.3. Medication history, laboratory hematology tests, and provocation test results of the patient with the *NLRP12* (A218V) mutation

The use of antibiotics (clinical cephalosporins, quinolones, macrolides) and antivirals during acute exacerbations was found to be ineffective. Colchicine did not relieve the fever or urticaria-like rash, instead prolonging the interictal period. A standard *NLRP12*-AID treatment regimen was administered to the patient, using prednisone 10 mg daily, cetirizine 10 mg daily, and methotrexate 12.5 mg weekly (Fig. 3A). The patient experienced relief from fever and a significant improvement in rash and arthralgia symptoms, indicating the effectiveness of this treatment.

The patient's medical records from December 2018 to September 2022 were retrospectively analyzed (Fig. 3B-Z). Hematologic findings showed that this *NLRP12* (A218V) patient's leukocyte (Fig. 3B), neutrophil (Fig. 3C), and monocyte (Fig. 3G) counts fluctuated cyclically and were apparently higher than the normal range during some of the acute attack periods. Neutrophil percentage (Fig. 3D) and monocyte percentage (Fig. 3H) fluctuated cyclically within the normal range of

values (except for a very few monitoring time points). Lymphocyte counts and percentages (Fig. 3E, F) fluctuated cyclically within the normal range except for a few time points. Eosinophil counts and percentages (Fig. 3I, J) fluctuated within the normal range and increased obviously during acute attacks. Basophil counts and percentages (Fig. 3K, L) fluctuated cyclically and were above the normal range during several acute attacks and interictal periods. Platelet counts (Fig. 3M) were fluctuated cyclically within normal limits. Based on the number of immune cells and platelets in the peripheral blood, we calculated four inflammatory markers, including NLR, PLR, LMR, and SII. NLR, PLR, and SII fluctuated cyclically and were elevated at some monitoring sites during acute attacks (Fig. 3N, O, and Q). LMR fluctuated cyclically, increasing or decreasing during acute attacks (Fig. 3P). Serum ALP (Fig. 3U), LDH (Fig. 3V) and CK (Fig. 3W) levels fluctuated periodically but were essentially in the normal range (except for a very few monitoring time points). Serum HDL-C was slightly below normal at some time points during the attack period (Fig. 3X). Serum ApoA1 levels were consistently lower than normal at all monitoring time points (Fig. 3Y). Serum 25(OH)D levels fluctuated at four different time points during the attack period (Fig. 3Z).

No viral, bacterial, fungal, or atypical pathogens were detected in the patient's blood during the seizure. Furthermore, the following laboratory test results were within normal limits for this patient, including antinuclear antibodies, anti-neutrophil cytoplasmic antibodies, anti-phospholipid antibodies, tumor biomarkers, erythrocyte sedimentation rate, and C-reactive protein. We did not find any significant abnormalities during echocardiography and bone puncture.

For a provocation test, a straight raised welt appeared on the skin at the five-minute mark (Fig. 3AA, AB), which then decreased slightly in size at 10 min (Fig. 3 AC), and almost completely disappeared after 30 min (Fig. 3 CE). These results suggest that the patient is susceptible to type I hypersensitivity reactions.

3.4. A218V mutation, similar with A218T and F402L, may reduce the ATP-binding affinity of the innate immune receptor *NLRP12*

At a single-cell transcriptome level, we found that *NLRP12* expression was highest in monocytes, followed by neutrophils and macrophages in PBMCs of healthy individuals (Fig. 4A-C). Inflammatory cytokines such as *IL18*, *CCL3*, and *TNFA* were higher in *NLRP12*-negative monocytes than in *NLRP12*-positive monocytes (Fig. 4D-F). *IL1B* expression levels were higher in *NLRP12*-negative monocytes than in *NLRP12*-positive monocytes, but the difference was not statistically significant (Fig. 4G). GSEA analysis revealed that *NLRP12* was associated with both immunosuppressive (Fig. 4H) and pro-inflammatory pathways (Fig. 4I), further suggesting its essential role in maintaining immune homeostasis at a single-cell transcriptome level.

Considering that ATP binding through the NACHT domain of *NLRP12* is critical for its inhibitory function 28, we explored the effects of A218 and other 10 NACHT-related mutations on protein stability and ATP-binding affinity of this protein (Fig. 4J-O). Eight of these 11 NACHT-related mutations, including mostly reported F402L, may destabilize the *NLRP12* protein, while A218V, P286L, and H304Y may have the opposite effect (Fig. 4K).

Molecular docking results showed that ATP binds in the NACHT domain surrounded by Leu153, Arg156, Tyr157, Thr158, Leu160, Ala218, Ala219, Gly220, and Ile221. Residues constituting the ATP-binding pocket include Gly222, Lys223, Ser224, Met225, His228, Arg253, Arg343, Phe365, Tyr373, Pro404, Trp408, Ile474, Asn498, Gln501, Ile513, His514, Leu515, Ser516, and Glu519. The volume of the ATP-binding pocket is 393.22 Å³, with Ala218 being one of the residues presented (Fig. 4L). The A218V, A218T, and F402L mutations enlarge the ATP-binding cavity, causing a volume increase to 550.40 Å³, 427.52 Å³ and 486.91 Å³ from 393.22 Å³, respectively. This results in weakened affinity between *NLRP12* and ATP, with a decrease in binding energy to -6.61 kcal/mol, -7.2 kcal/mol, and -6.87 kcal/mol in A218V, A218T,

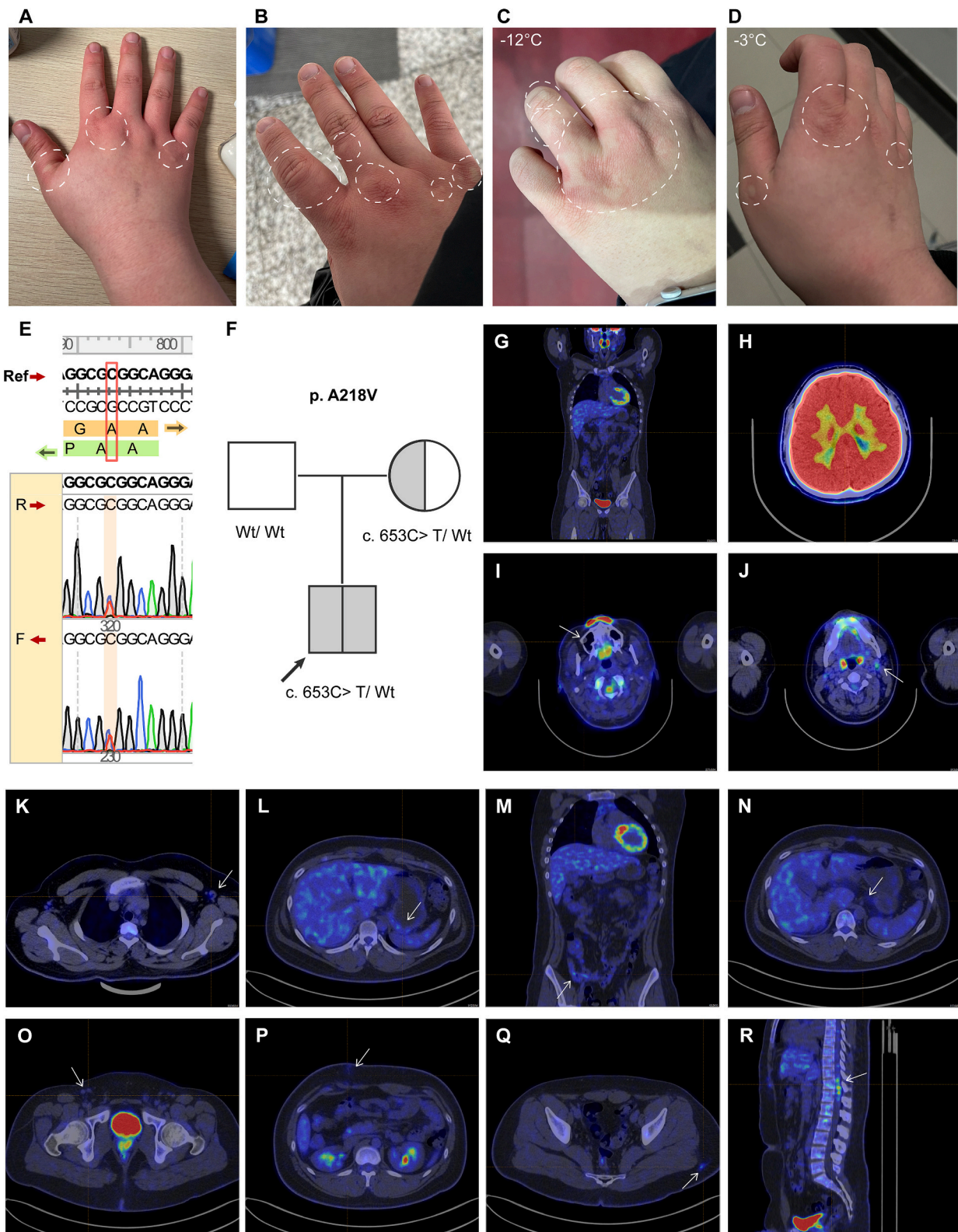
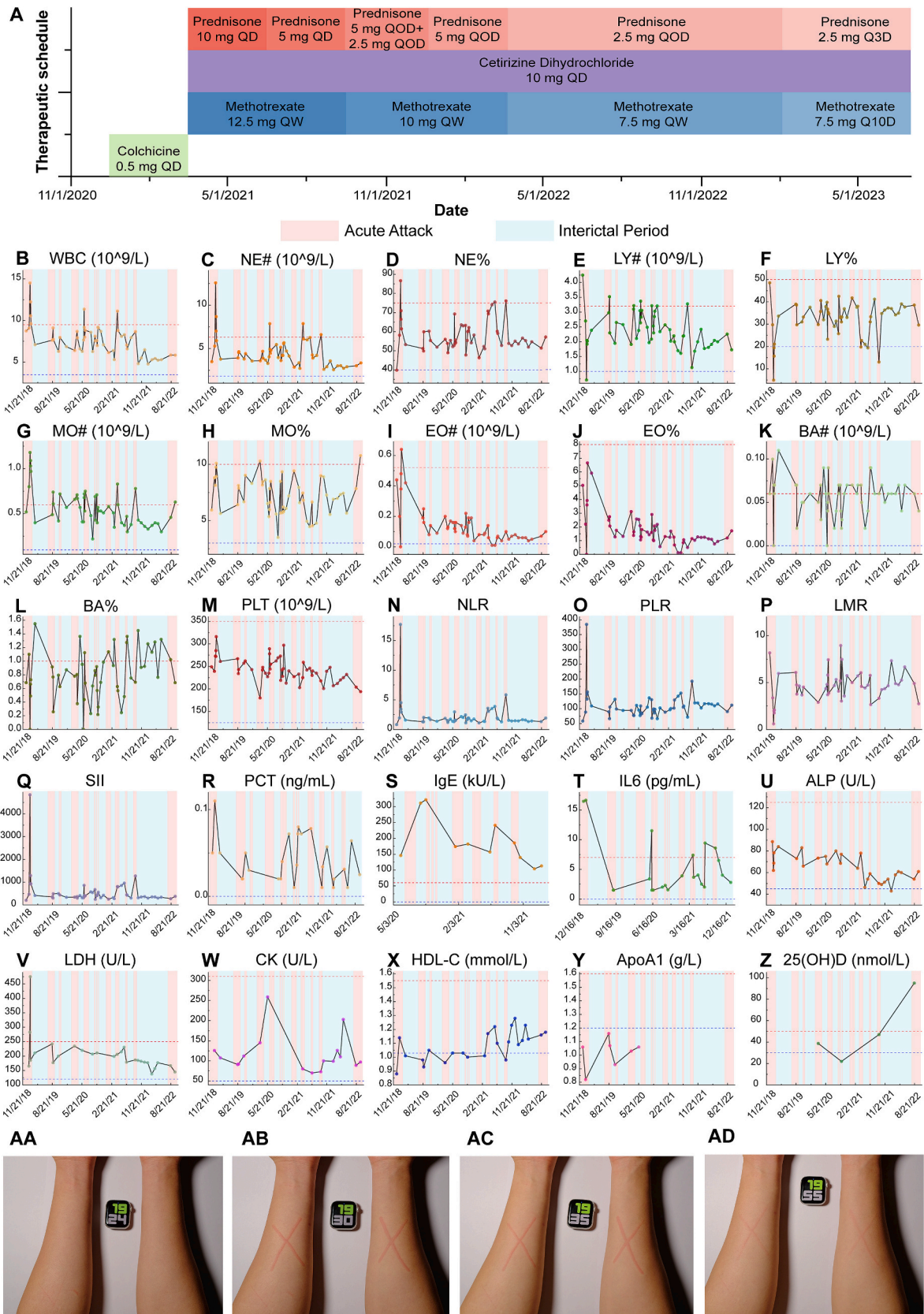


Fig. 2. Clinical characteristics, Sanger sequencing results, and imaging manifestations of the patient with the NLRP12 (A218V) mutation. The patient reported pain and swelling (A) in the finger joints and a rash (B) during acute episodes or after exposure to cold. After cold induction, the patient presented with an erythematous and urticarial skin rash (C–D). Sanger sequencing confirmed the heterozygous c.653C > T mutation in both the patient and his mother, which resulted in the substitution of the amino acid alanine (E–F), compared to the *NLRP12* reference sequence, as shown in both forward and reverse sequencing. The PET/CT scan was performed after a six-hour fast, during which the patient abstained from sugary beverages and achieved normal blood glucose levels. No sedatives were administered. The patient received an intravenous injection of 0.15 mCi/kg of ^{18}F -FDG and then underwent whole-body PET/CT imaging after 60 min of uninterrupted rest. Imaging covered various areas, including the whole body (G), cerebral region (H), maxillary sinus (I), neck (J), axilla (K), stomach (L), intestine (M), abdominal cavity (N), inguinal region (O), right lower abdomen (P), buttocks (Q), and bone marrow (R).



(caption on next page)

Fig. 3. Medication history, long-term laboratory hematology tests, and a provocation test for the patient with the NLRP12 (A218V) mutation. The patient received colchicine treatment on December 15, 2020, and was subsequently switched to prednisone, methotrexate, and cetirizine from March 16, 2021, to the present (A). The long-term monitoring of laboratory parameters extends from December 2018 (active phase) to September 2022. All laboratory results, including those obtained during the attack and interval periods, were collected for the patient. The following parameters were monitored, including white blood cell count (WBC, B), neutrophil count (NE#, C), neutrophil percentage (NE%, D), lymphocyte count (LY#, E), lymphocyte percentage (LY%, F), monocyte count (MO#, G), monocyte percentage (MO%, H), eosinophil count (EO#, I), eosinophil percentage (EO%, J), basophil count (BA#, K), basophil percentage (BA%, L), platelets (PLT, M), neutrophil-to-lymphocyte ratio (NLR, N), platelet-to-lymphocyte ratio (PLR, O), lymphocyte-to-monocyte ratio (LMR, P), systemic immune-inflammation index (SII, Q), PCT (R), IgE (S), IL6 (T), alkaline phosphatase (ALP, U), lactate dehydrogenase (LDH, V), creatine kinase (CK, W), high-density lipoprotein cholesterol (HDL—C, X), apolipoprotein A1 (ApoA1, Y), and 25-hydroxyvitamin D (25(OH)D, Z). To diagnose a provocation test, a positive reaction was observed when the volar aspect of the patient's forearm was stroked with a tongue depressor on normal skin (AA). A straight raised welt appeared on the skin at the five-minute mark (AB), which then decreased slightly in size at 10 min (AC) and almost completely disappeared at 30 min (AD). QD: once daily; QOD: every other day; Q3D: every three days; QW: once a week; Q10D: Every 10 days.

and F402L mutants, respectively (Fig. 4K-O).

4. Discussion

Little is known about *NLRP12*-AID due to its rarity. In this study, we report a case of *NLRP12*-AID caused by *NLRP12* (A218V) mutation. We posit that this mutation weakens the binding between *NLRP12* and ATP, lessening its capacity to dampen the inflammatory response which prompts typical symptoms of AID (Fig. 5).

NLRP12-AID patients have primarily exhibited clinical symptoms such as cold-induced periodic fever, elevated inflammatory markers during acute attacks, multiple urticaria-like rashes and other skin symptoms, as well as joint swelling and pain, and other musculoskeletal symptoms [3,25]. The patient with *NLRP12* (A218V) mutation consistently exhibited clinical symptoms including periodic fever, joint pain, and a rash resembling cold-induced urticaria, along with heightened inflammatory markers during acute episodes. Additionally, the serum IgE levels of the patient with *NLRP12* (A218V) mutation consistently exceeded normal reference values, and the eosinophil levels increased obviously during acute attacks. Basophil levels fluctuated cyclically and were above the normal range during acute attacks and even during several interlertic periods. These results suggest that the patient may undergo allergic responses during acute episodes, with the emergence of urticaria-like eruptions caused by exposure to cold, supporting the use of antihistamine medications. Decreased levels of HDL-C and ApoA1 have been reported in patients with some autoimmune diseases, such as juvenile-onset systemic lupus erythematosus. In this study, we demonstrated decreased serum levels of HDL-C and ApoA1 in a novel case of *NLRP12*-AID. These findings highlight the importance of lipid abnormalities in autoinflammatory and autoimmune diseases. Inflammatory markers such as NLR, PLR, and SII, exhibited a periodic increasing trend, indicating that the patient exhibits a chronic inflammatory response periodically. Furthermore, PET/CT imaging revealed extensive chronic inflammation in multiple tissue sites of the patient with *NLRP12* (A218V) mutation. Previous studies have shown that combination therapy with corticosteroids, antihistamines, and DMARDs is effective in alleviating symptoms in most *NLRP12*-AID patients. In this study, the patient received a treatment regimen of prednisone, methotrexate, and cetirizine after the empirical treatment with colchicine failed. This regimen alleviated clinical symptoms and improved the patient's quality of life.

NLRP12 plays both pro-inflammatory and anti-inflammatory roles [29,30], which is further supported by a single-cell level GSEA analysis in this study. Recently, the role of *NLRP12* as a negative immune modulator has received increasing attention. Based on single-cell RNA sequencing on PBMC of healthy individuals, we found that *NLRP12* is predominantly expressed in monocytes. We further demonstrated at the single-cell level that *NLRP12*-expressing monocytes exhibit lower expression levels of *TNFA*, *IL18*, and *CCL3* than *NLRP12*-negative monocytes, thus suggesting an anti-inflammatory role of *NLRP12* under physiological conditions. *NLRP12* can suppress the body's inflammatory response through two mechanisms. On one hand, *NLRP12* reduces excessive phosphorylation of interleukin-1 receptor-associated kinase 1

mediated by Toll-like receptor, which allows it to suppress the IRAK-1 signaling pathway [31]. On the other hand, *NLRP12* inhibits the NF- κ B pathway by binding to NF- κ B-inducing kinase (NIK), which destabilizes NIK and blocks the conversion of NF- κ B2/p100 into p52 [32]. These pathways downstream of *NLRP12* suggest potential targets for the treatment of *NLRP12*-AID. In the future, the aberrant function of *NLRP12* mutants may be corrected by gene editing techniques such as CRISPR/Cas9, leading to a cure for *NLRP12*-AID.

In 2016, Xia et al. reported a nonsense mutation (W408X) within the NACHT domain of *NLRP12* that disrupted the integrity of this protein [26]. As we summarized, most reported *NLRP12* mutations occur in the NACHT domain, while a few are in its PYRIN domain. A218V mutation was also located in the NACHT domain of *NLRP12*. ATP binding by the NACHT domain is critical for the inhibitory function of *NLRP12* [28,33]. The A218V missense mutation in *NLRP12* is situated in its ATP binding pocket. F402L is by far the most widely reported pathogenic mutation of *NLRP12*-AID that causes the most typical clinical symptoms. We conclude by computational structure analysis that both A218V and F402L mutations causing *NLRP12*-AID are the result of a decrease in the NACHT domain binding ATP ability of the *NLRP12* protein, which may be due to an enlarged ATP pocket caused by mutations. Furthermore, in contrast to F402L, which may decrease *NLRP12* protein stability, the A218V mutation may even upregulate it. YE et al. illustrate the fundamental role of *NLRP12* binding to ATP in inhibiting NF- κ B activation and inflammatory signals. They also observed a notable increase in proinflammatory cytokine production in monocytes when the ATP binding site of *NLRP12* was defective [33]. Taken together, we hypothesized that the *NLRP12* (A218V) mutation may contribute to the development and progression of *NLRP12*-AID by attenuating the binding between the NACHT structural domain of the *NLRP12* protein and ATP in myeloid cells (especially monocytes), which in turn attenuates its inhibitory effect and thus leads to the development of *NLRP12*-AID. Our findings from computational predictions suggest that ATP-based therapeutic approaches may have some potential in the treatment of auto-inflammatory diseases caused by some specific *NLRP12* mutations. The combination of ATP-based therapeutic approaches with existing anti-inflammatory agents also deserves further investigation.

There are two major limitations of this study. First, due to the rarity of *NLRP12*-AID, we presented only one case of the *NLRP12* (A218V) mutation. Additional cases featuring the A218V mutation would enhance the robustness and generalizability of the results. Second, we used bioinformatics analyses to explore the potential mechanisms underlying the pathogenesis of *NLRP12*-AID from the perspective of gene expression and structure of *NLRP12*. These results from computational predictions require further functional experimental validation.

5. Conclusion

In summary, we present the case of a 21-year-old male patient of Han Chinese descent diagnosed with *NLRP12*-AID resulting from a missense mutation (A218V) in *NLRP12*. Bioinformatic analyses suggested that the *NLRP12* (A218V) mutation may disrupt the immunoregulatory role of this protein by attenuating its binding affinity for ATP. Our findings

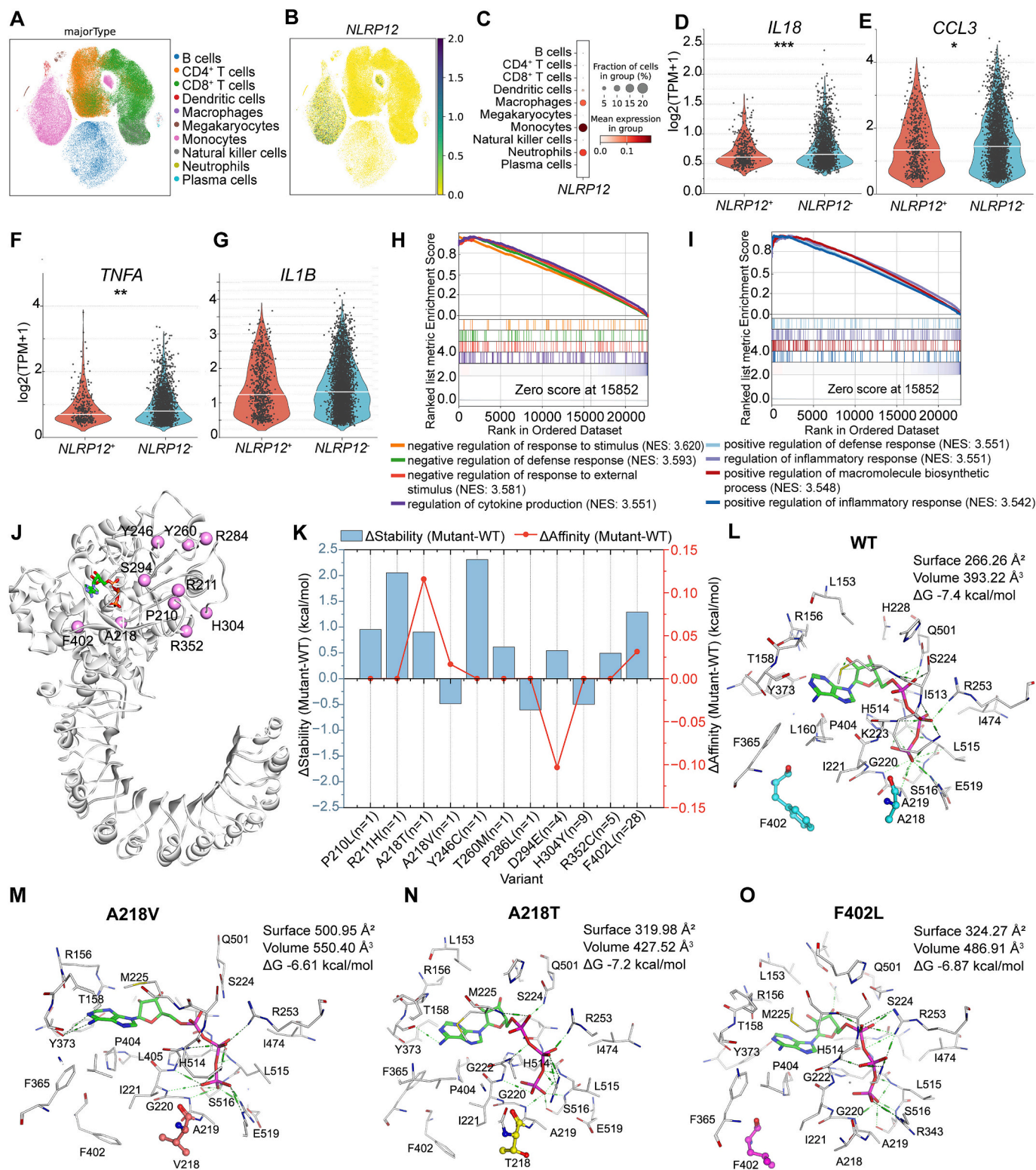


Fig. 4. Single-cell expression pattern of NLRP12 in healthy human PBMC and prediction of the ATP binding capacity of NLRP12 mutants by molecular docking. The GSE158055 dataset was obtained from the GEO database. (A) Cell subpopulation distribution. (B–C) The expression pattern of NLRP12 among these cell subpopulations. (D–G) Comparison of *IL18* (D), *CCL3* (E), *TNFA* (F), and *IL1B* (G) between NLRP12-positive and NLRP12-negative monocytes. (H–I) Both pro- and anti-immune pathways were enriched in NLRP12 positive cells compared to NLRP12 negative cells. (J) The structure of wild-type NLRP12. (K) Prediction of the effects of 11 point mutations located in the NACHT domain on the stability (red line) and ATP-binding capacity (blue bar) of the NLRP12 protein. (L–O) ATP-binding cavity of wild-type NLRP12 (L), and A218V (M), A218T (N), F402L mutants (O). The Design module of MOE2020.09 was employed to construct the A218V mutant. The binding pocket volume was calculated using Protein Plus, and the PRODIGY server was utilized to predict the binding energy between the protein and ATP. * $P < 0.05$, ** $P < 0.01$, *** $P < 0.001$. (For interpretation of the references to colour in this figure legend, the reader is referred to the web version of this article.)

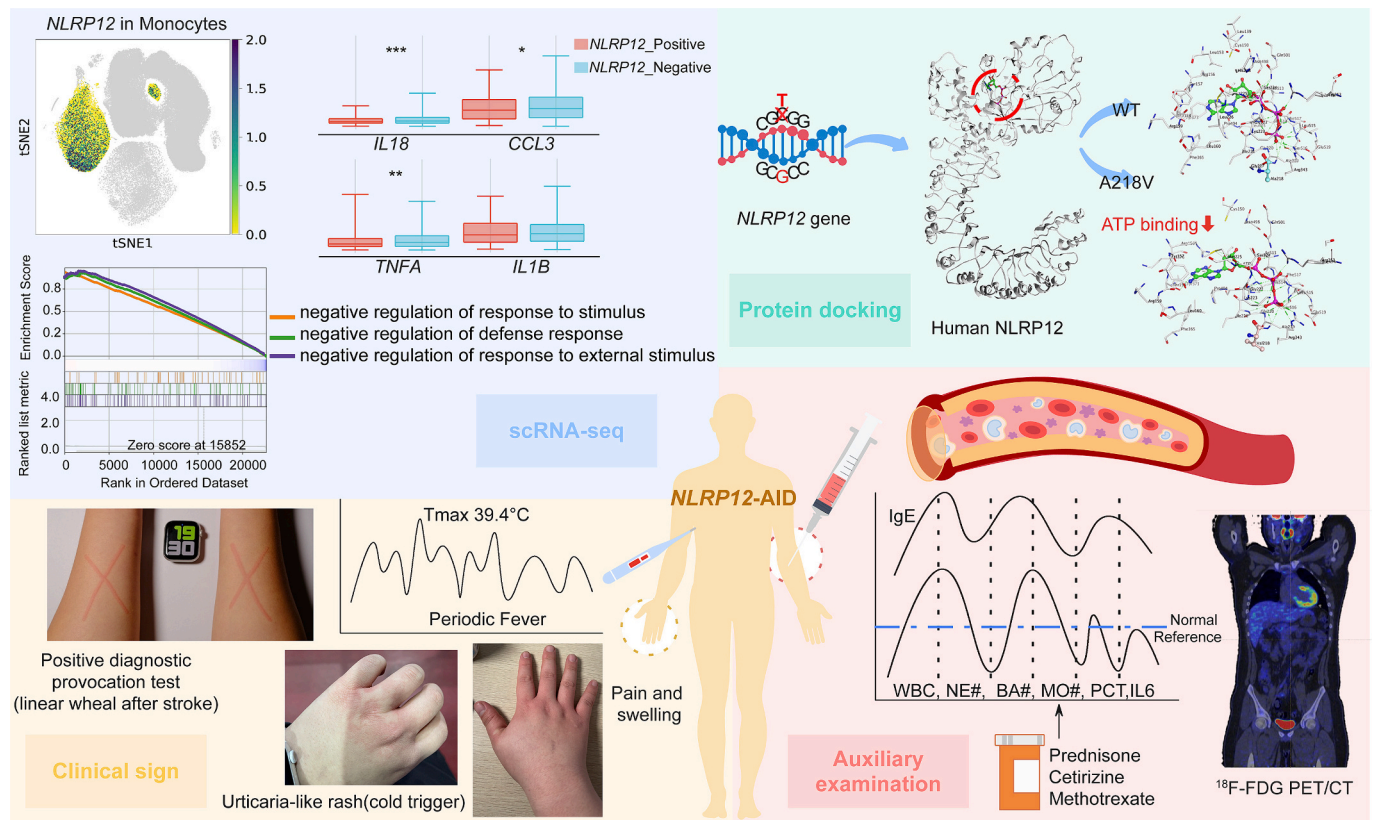


Fig. 5. A schematic diagram of the possible pathogenic mechanisms of the NLRP12 (A218V) mutation.

contribute to the understanding of the clinical symptoms, heterogeneity, and pathogenesis of the rare disease *NLRP12*-AID and suggest a potential role for ATP-based therapy in *NLRP12*-AID triggered by A218V, A218T, or F402L mutations.

Funding

This study was supported by the Fundamental Research Funds for the Central Universities of China (2632022ZD10).

CRediT authorship contribution statement

Zhonghua Li: Formal analysis, Investigation, Visualization, Writing – original draft. **Qi Zhi:** Formal analysis, Investigation, Visualization. **Jiahuang Li:** Funding acquisition, Methodology, Supervision. **Bo Zhu:** Conceptualization, Funding acquisition, Methodology, Supervision, Writing – review & editing.

Declaration of competing interest

The authors declare that they have no competing interests.

Data availability

The single-cell transcriptome data used to support the findings of this study are available from the GEO database (<https://www.ncbi.nlm.nih.gov/geo/>).

Acknowledgment

We are grateful to the patient and his family, whose cooperation made this study possible, and to Prof. Dr. Min Shen from the Department of Rheumatology at Peking Union Medical College Hospital, for her

contribution to clinical data acquisition.

Appendix A. Supplementary data

Supplementary data to this article can be found online at <https://doi.org/10.1016/j.clim.2024.110278>.

References

- [1] A. Moreira, B. Torres, J. Peruzzo, A. Mota, K. Eyerich, J. Ring, Skin symptoms as diagnostic clue for autoinflammatory diseases, *An. Bras. Dermatol.* 92 (1) (2017) 72–80, <https://doi.org/10.1590/abd1806-4841.20175208>. Jan-Feb.
- [2] H.F. Wang, NLRP12-associated systemic autoinflammatory diseases in children, *Pediatr. Rheumatol. Online J.* 20 (1) (Feb 5 2022) 9, <https://doi.org/10.1186/s12969-022-00669-8>.
- [3] M. Shen, L. Tang, X. Shi, X. Zeng, Q. Yao, NLRP12 autoinflammatory disease: a Chinese case series and literature review, *Clin. Rheumatol.* 36 (7) (2017) 1661–1667, <https://doi.org/10.1007/s10067-016-3410-y>. Jul.
- [4] N. Jacob, S.S. Dasharathy, V. Bui, et al., Generalized cytokine increase in the setting of a multisystem clinical disorder and carcinoid syndrome associated with novel NLRP12 variant, *Dig. Dis. Sci.* 64 (8) (2019) 2140–2146, <https://doi.org/10.1007/s10620-019-05525-6>. Aug.
- [5] S. Antunes-Duarte, A. Marcos-Pinto, L.E. French, H. Kutzner, L. Soares-de-Almeida, NLRP12 and IL36RN mutations in a Portuguese woman with autoinflammatory syndrome, *JAAD Case Rep.* 26 (2022) 91–94, <https://doi.org/10.1016/j.jcdr.2022.06.011>. Aug.
- [6] A.Y. Ayla, H. Eren, J. Zare, et al., A rare case of an NLRP12-associated autoinflammatory disease, *Eur. J. Med. Genet.* 64 (4) (2021) 104168, <https://doi.org/10.1016/j.ejmg.2021.104168>. Apr.
- [7] O. Basaran, N. Uncu, N. Cakar, et al., C3 glomerulopathy in NLRP12-related autoinflammatory disorder: case-based review, *Rheumatol. Int.* 38 (8) (2018) 1571–1576, <https://doi.org/10.1007/s00296-018-4092-3>. Aug.
- [8] S. Borghini, S. Tassi, S. Chiesa, et al., Clinical presentation and pathogenesis of cold-induced autoinflammatory disease in a family with recurrence of an NLRP12 mutation, *Arthritis Rheum.* 63 (3) (2011) 830–839, <https://doi.org/10.1002/art.30170>. Mar.
- [9] S. Borte, M.H. Celiksoy, V. Menzel, et al., Novel NLRP12 mutations associated with intestinal amyloidosis in a patient diagnosed with common variable immunodeficiency, *Clin. Immunol.* 154 (2) (2014) 105–111, <https://doi.org/10.1016/j.clim.2014.07.003>. Oct.

- [10] S. Chen, Z. Li, X. Hu, et al., Rare mutations in NLRP3 and NLRP12 associated with familial cold autoinflammatory syndrome: two Chinese pedigrees, *Clin. Rheumatol.* 41 (11) (2022) 3461–3470, <https://doi.org/10.1007/s10067-022-06292-y>. Nov.
- [11] M. Cichon, P. Zielinska, J.M. Zaucha, E. Zarzycka, M. Trzeciak, Cold-induced urticaria-like lesions related to NLRP-12 mutation, *J. Eur. Acad. Dermatol. Venereol.* (Feb 14 2023), <https://doi.org/10.1111/jdv.18969>.
- [12] C. De Pieri, J. Vuch, E. Athanasakis, et al., F402L variant in NLRP12 in subjects with undiagnosed periodic fevers and in healthy controls, *Clin. Exp. Rheumatol.* 32 (6) (2014) 993–994. Nov-Dec.
- [13] F. Del Porto, N. Cifani, M. Proietta, et al., NLRP12 gene mutations and auto-inflammatory diseases: ever-changing evidence, *Rheumatology (Oxford)* 59 (11) (2020) 3129–3136, <https://doi.org/10.1093/rheumatology/keaa304>. Nov 1.
- [14] C. Eijkelboom, N.M. Ter Haar, J. Frenkel, M. Gattorno, Response to: 'Novel NLRP12 variant presenting with familial cold autoimmunity syndrome phenotype' by Gupta et al. *Ann. Rheum. Dis.* 80 (7) (2021) e118, <https://doi.org/10.1136/annrheumdis-2019-216184>. Jul.
- [15] K. Ghosh, K. Mishra, A. Shah, P. Patel, S. Shetty, Novel deleterious sequence change in the NLRP12 gene in a child with the autoinflammatory syndrome, joint hypermobility and cutis Laxa from India, *Mediterr J Hematol Infect Dis.* 11 (1) (2019) e2019018, <https://doi.org/10.4084/MJHID.2019.018>.
- [16] Y. Hua, D. Wu, M. Shen, K. Yu, W. Zhang, X. Zeng, Phenotypes and genotypes of Chinese adult patients with systemic autoinflammatory diseases, *Semin. Arthritis Rheum.* 49 (3) (2019) 446–452, <https://doi.org/10.1016/j.semarthrit.2019.05.002>. Dec.
- [17] I. Jéru, P. Duquesnoy, T. Fernandes-Alnemri, et al., Mutations in NALP12 cause hereditary periodic fever syndromes, *Proc. Natl. Acad. Sci. USA* 105 (5) (Feb 5 2008) 1614–1619, <https://doi.org/10.1073/pnas.0708616105>.
- [18] I. Jeru, G. Le Borgne, E. Cochet, et al., Identification and functional consequences of a recurrent NLRP12 missense mutation in periodic fever syndromes, *Arthritis Rheum.* 63 (5) (2011) 1459–1464, <https://doi.org/10.1002/art.30241>. May.
- [19] M.M. Kostik, E.N. Suspitsin, M.N. Guseva, et al., Multigene sequencing reveals heterogeneity of NLRP12-related autoinflammatory disorders, *Rheumatol. Int.* 38 (5) (2018) 887–893, <https://doi.org/10.1007/s00296-018-4002-8>. May.
- [20] P.A. Ledesma, J.C. Guerra, M. Burbano, P. Procel, L.A. Pedroza, Whole exome sequencing in a child with acute disseminated encephalomyelitis, optic neuritis, and periodic fever syndrome: a case report, *J. Med. Case Rep.* 13 (1) (2019) 368, <https://doi.org/10.1186/s13256-019-2305-3>. Dec 14.
- [21] D. Levy, A. Mariotte, A. DeCauwer, et al., Contrasting role of NLRP12 in autoinflammation: evidence from a case report and mouse models, *RMD Open* 7 (3) (2021), <https://doi.org/10.1136/rmdopen-2021-001824>. Oct.
- [22] M. Rusmini, S. Federici, F. Caroli, et al., Next-generation sequencing and its initial applications for molecular diagnosis of systemic auto-inflammatory diseases, *Ann. Rheum. Dis.* 75 (8) (2016) 1550–1557, <https://doi.org/10.1136/annrheumdis-2015-207701>. Aug.
- [23] A. Vitale, D. Rigante, M.C. Maggio, et al., Rare NLRP12 variants associated with the NLRP12-autoinflammatory disorder phenotype: an Italian case series, *Clin Exp Rheumatol.* May-Jun 31 (3 Suppl 77) (2013) 155–156.
- [24] J. Wang, Q. Zhang, L. Xu, et al., A case of episodic and refractory arthritis due to a novel variant of NLRP12, *Ann. Rheum. Dis.* 81 (2) (2022) e33, <https://doi.org/10.1136/annrheumdis-2020-217023>. Feb.
- [25] W. Wang, Y. Zhou, L.Q. Zhong, et al., The clinical phenotype and genotype of NLRP12-autoinflammatory disease: a Chinese case series with literature review, *World J. Pediatr.* 16 (5) (2020) 514–519, <https://doi.org/10.1007/s12519-019-00294-8>. Oct.
- [26] X. Xia, C. Dai, X. Zhu, et al., Identification of a novel NLRP12 nonsense mutation (Trp408X) in the extremely rare disease FCAS by exome sequencing, *PLoS One* 11 (6) (2016) e0156981, <https://doi.org/10.1371/journal.pone.0156981>.
- [27] X. Yang, B. Zhao, Y. Liao, Analysis on misdiagnosis of a case of novel variant of NLRP12, *Ann. Rheum. Dis.* 82 (1) (2023) e26, <https://doi.org/10.1136/annrheumdis-2020-218422>. Jan.
- [28] J.A. MacDonald, C.P. Wijekoon, K.C. Liao, D.A. Muruve, Biochemical and structural aspects of the ATP-binding domain in inflammasome-forming human NLRP proteins, *IUBMB Life* 65 (10) (2013) 851–862, <https://doi.org/10.1002/iub.1210>. Oct.
- [29] P. Broz, V.M. Dixit, Inflammasomes: mechanism of assembly, regulation and signalling, *Nat. Rev. Immunol.* 16 (7) (2016) 407–420, <https://doi.org/10.1038/nri.2016.58>. Jul.
- [30] M. Gharagozloo, K.V. Gris, T. Mahvelati, A. Amrani, J.R. Lukens, D. Gris, NLR-dependent regulation of inflammation in multiple sclerosis, *Front. Immunol.* 8 (2017) 2012, <https://doi.org/10.3389/fimmu.2017.02012>.
- [31] K.L. Williams, J.D. Lich, J.A. Duncan, et al., The CATERPILLER protein monarch-1 is an antagonist of toll-like receptor-, tumor necrosis factor alpha-, and mycobacterium tuberculosis-induced pro-inflammatory signals, *J. Biol. Chem.* 280 (48) (2005) 39914–39924, <https://doi.org/10.1074/jbc.M502820200>. Dec 2.
- [32] J.D. Lich, K.L. Williams, C.B. Moore, et al., Monarch-1 suppresses non-canonical NF-kappaB activation and p52-dependent chemokine expression in monocytes, *J. Immunol.* 178 (3) (Feb 1 2007) 1256–1260, <https://doi.org/10.4049/jimmunol.178.3.1256>.
- [33] Z. Ye, J.D. Lich, C.B. Moore, J.A. Duncan, K.L. Williams, J.P. Ting, ATP binding by monarch-1/NLRP12 is critical for its inhibitory function, *Mol. Cell. Biol.* 28 (5) (2008) 1841–1850, <https://doi.org/10.1128/mcb.01468-07>. Mar.